

Poisson-Gamma Dynamical Systems with Non-Stationary Transition Dynamics

Jiahao Wang¹, Sikun Yang², Heinz Koepl³, Xiuzhen Cheng¹, Pengfei Hu¹, Guoming Zhang¹

¹School of Computer Science and Technology, Shandong University

²School of Computing and Information Technology, Great Bay University

³Department of Electrical Engineering and Information Technology, Technische Universität Darmstadt

Abstract

Bayesian methodologies for handling count-valued time series have gained prominence due to their ability to infer interpretable latent structures and to estimate uncertainties, and thus are especially suitable for dealing with *noisy* and *incomplete* count data. Among these Bayesian models, Poisson-Gamma Dynamical Systems (PGDSs) are proven to be effective in capturing the evolving dynamics underlying observed count sequences. However, the state-of-the-art PGDS still falls short in capturing the *time-varying* transition dynamics that are commonly observed in real-world count time series. To mitigate this limitation, a non-stationary PGDS is proposed to allow the underlying transition matrices to evolve over time, and the evolving transition matrices are modeled by sophisticatedly-designed Dirichlet Markov chains. Leveraging Dirichlet-Multinomial-Beta data augmentation techniques, a fully-conjugate and efficient Gibbs sampler is developed to perform posterior simulation. Experiments show that, in comparison with related models, the proposed non-stationary PGDS achieves improved predictive performance due to its capacity to learn non-stationary dependency structure captured by the time-evolving transition matrices.

1 Introduction

In recent years, there has been an increasing interest in modeling count time series. For instance, some previous works [Blei and Lafferty, 2006; Wang and McCallum, 2006; Jähnichen *et al.*, 2018] are concerned with how to learn the evolving topics behind text corpus (frequencies of words) over time. Some works [Sheldon and Dietterich, 2011; Raymer *et al.*, 2013; Wilson, 2017; Wanner, 2021] try to predict global immigrant trends underlying international population movements. Count time series are often *overdispersed*, *sparse*, *high-dimensional*, and thus can not be well modeled by widely used dynamic models such as linear dynamical systems [Kalman, 1960; Ghahramani and Roweis, 1998]. Recently, many works [Zhou and Carin, 2012; Zhou and Carin, 2015; Schein *et al.*, 2015; Schein *et al.*, 2016b; Schein *et al.*, 2016a; Acharya *et al.*, 2015; Schein *et al.*,

2019] prefer to choose distributions of the gamma-Poisson family to build their hierarchical Bayesian models. In particular, these models enjoy strong explainability and can estimate uncertainty especially when the observations are *noisy* and *incomplete*. Among these works, Poisson-Gamma Dynamical Systems (PGDSs) [Schein *et al.*, 2016b] received a lot of attention because PGDS can learn how the latent dimensions excite each other to capture complicated dynamics in observed count series. For instance, a very inspiring research paper may motivate other researchers to publish papers on related topics [Chang and Blei, 2009]. The outbreak of COVID-19 in one state, may lead to the rapid rising of COVID-19 cases in the nearby states and vice versa [Unwin *et al.*, 2020]. In particular, PGDS can be efficiently learned with a tractable Gibbs sampling scheme via Poisson-Logarithmic data augmentation and marginalization technique [Zhou and Carin, 2015]. Due to its strong flexibility, PGDS achieves better performance in predicting missing entities and future observations, compared with related models [Ghahramani and Roweis, 1998; Acharya *et al.*, 2015].

Despite these advantages, PGDS still can not capture the time-varying transition dynamics underlying observed count sequences, which are commonly observed in real-world scenarios [Winkelmann, 2008]. For instance, during the initial stage of the COVID-19 pandemic, the worldwide counts of infectious patients were significantly affected by various local policies, government interventions, and emergent events [Grossman *et al.*, 2020; Team, 2021; Feng *et al.*, 2021]. The cross transition dynamics among the different monitoring areas were also evolving as the corresponding policies and interventions changed over time. Hence, PGDS unavoidably makes a certain amount of approximation error in capturing the aforementioned non-stationary count time series, using a *time-invariant* transition kernel.

To mitigate this limitation, Non-Stationary Poisson-Gamma Dynamical Systems (NS-PGDSs), a novel kind of Poisson-gamma dynamical systems with non-stationary transition dynamics are developed. More specifically, NS-PGDS captures the evolving transition dynamics by sophisticatedly designed Dirichlet Markov chains. Via the Dirichlet-Multinomial-Beta data augmentation strategy, the Non-Stationary Poisson-Gamma Dynamical Systems can be inferred with a conjugate-yet-efficient Gibbs sampler. Our contributions are summarized as follows:

- We propose a Non-Stationary Poisson-Gamma Dynamical System (NS-PGDS), a novel Poisson-gamma dynamical system with time-evolving transition matrices that can well capture non-stationary transition dynamics underlying observed count series.
- Three sophisticated Dirichlet Markov chains are dedicated to improving the flexibility and expressiveness of NS-PGDSs, for capturing the complex transition dynamics behind sequential count data.
- Fully-conjugate-yet-efficient Gibbs samplers are developed via Dirichlet-Multinomial-Beta augmentation techniques to perform posterior simulation for the proposed Dirichlet Markov chains.
- Extensive experiments are conducted on four real-world datasets, to evaluate the performance of the proposed NS-PGDS in predicting missing and future unseen observations. We also provide exploratory analysis to demonstrate the explainable latent structure inferred by the proposed NS-PGDS.

2 Preliminaries

Let $\mathbf{y}^{(t)} = [y_1^{(t)}, \dots, y_V^{(t)}]^T \in \mathbb{N}_0^V$ be a vector of nonnegative count valued observations at time t . To capture the latent dynamics underlying count sequences, some previous works [Han *et al.*, 2014; Kalantari and Zhou, 2020] model the observations as

$$\mathbf{y}^{(t)} = p(\mathbf{z}^{(t)}), \quad \mathbf{z}^{(t)} = f^{-1}(\mathbf{x}^{(t)}),$$

where $p(\cdot)$ is the observation likelihood function, and $f(\cdot)$ is a link function that maps the parameters of observation component to continuous-valued latent variables $\mathbf{x}^{(t)} \in \mathbb{R}^K$. The latent factor $\mathbf{x}^{(t)}$ evolves over time according to a linear dynamical system given by $\mathbf{x}^{(t)} \sim \mathcal{N}(\mathbf{A}\mathbf{x}^{(t-1)}, \mathbf{\Lambda}^{-1})$, where \mathbf{A} is the state transition matrix of size $K \times K$, and $\mathbf{\Lambda} = \text{diag}(\lambda_1, \dots, \lambda_K)$ is the inverse covariance matrix with λ_k^{-1} determining the variance of k -th latent dimension. Han *et al.* [2014] adopted the Extended Rank likelihood function to model count observations using LDS with time complexity $\mathcal{O}((K+V)^3)$, which prevents it from practical applications for analyzing large-scale count data.

Recently, Acharya *et al.* [2015] and Schein *et al.* [2016b; 2019] developed Poisson-gamma family models for sequential count observations. Gamma Process Dynamic Poisson Factor Analysis (GP-DPFA) [Acharya *et al.*, 2015] models count data as $y_v^{(t)} \sim \text{Pois}(\sum_{k=1}^K \lambda_k \phi_{vk} \theta_k^{(t)})$, where $\theta_k^{(t)}$ represents the strength of k -th latent factor at time t , and ϕ_{vk} captures the involvement degree of k -th factor to v -th observed dimension. To ensure the model identifiability, we can impose a restriction as $\sum_v \phi_{vk} = 1$, and thus place a Dirichlet prior over $\phi_{\mathbf{k}} = [\phi_{1k}, \dots, \phi_{V_k}]^T$ as $\phi_{\mathbf{k}} \sim \text{Dir}(\epsilon_0, \dots, \epsilon_0)$. To capture the underlying dynamics, the latent factor $\theta_k^{(t)}$ evolves over time according to a gamma Markov chain as $\theta_k^{(t)} \sim \text{Gam}(\theta_k^{(t-1)}, c_t)$, where c_t is the

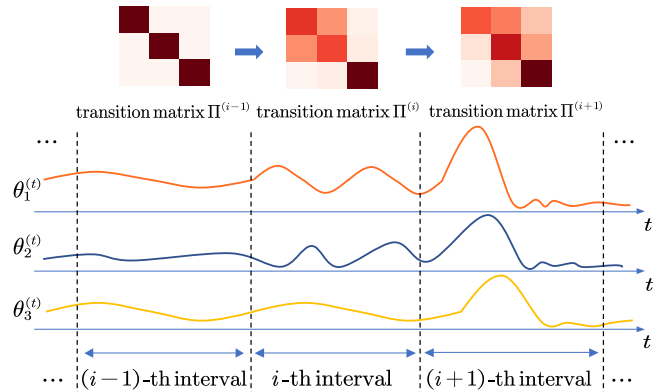


Figure 1: An example illustrates the Poisson-gamma dynamical systems with non-stationary transition kernels. The three gamma dynamic processes independently evolve over time during the $(i-1)$ -th interval. During i -th interval, $\theta_1^{(t)}$ and $\theta_2^{(t)}$ gradually starts to interact with each other while $\theta_3^{(t)}$ remains independent to the other two dimensions. During $(i+1)$ -th interval all the three latent components start to interact with each other.

rate parameter of the gamma distribution to control the variance of gamma Markov chains. Although GP-DPFA can well fit one-dimensional count sequences, it fails to learn how the latent dimensions interact with each other.

To address this concern, Schein *et al.* [2016b] developed Poisson-gamma dynamical systems to capture the underlying transition dynamics. In particular, $\theta_k^{(t)}$ evolves over time as $\theta_k^{(t)} \sim \text{Gam}(\tau_0 \sum_{k_2=1}^K \pi_{kk_2} \theta_{k_2}^{(t-1)}, \tau_0)$, where π_{kk_2} represents how k_2 -th latent factor excites the k -th latent factor at next time step, and $\sum_{k_2=1}^K \pi_{kk_2} = 1$.

3 Non-Stationary Poisson-Gamma Dynamical Systems

Real-world count time sequences are often *non-stationary* because the external interventional environments are always changing over time. The stationary PGDS with a time-invariant transition kernel fails to capture such time-varying transition dynamics. For instance, the transition dynamics behind COVID-19 infectious processes are time-varying, and highly affected by various interventional policies. Hence, to mitigate this limitation, we model the count sequences as

$$y_v^{(t)} \sim \text{Pois}(\delta^{(t)} \sum_{k=1}^K \phi_{vk} \theta_k^{(t)}),$$

in which, the latent factors are specified by

$$\theta_k^{(t)} \sim \text{Gam}(\tau_0 \sum_{k_2=1}^K \pi_{kk_2}^{(t-1)} \theta_{k_2}^{(t-1)}, \tau_0), \quad (1)$$

where the multiplicative term $\delta^{(t)} \sim \text{Gam}(\epsilon_0, \epsilon_0)$ and the transition matrices are time-varying as $\mathbf{\Pi}^{(t)} \equiv [\pi_{kk_2}^{(t)}]_{k,k_2=1}^K$.

As shown in Figure 1, to model the time-varying transition dynamics, we assume the whole time interval can be divided into I equally-spaced sub-intervals. The transition kernel behind complicated dynamic counts is assumed to be *static* within each sub-interval, while evolving over sub-intervals, to capture non-stationary behaviours. In another word, the

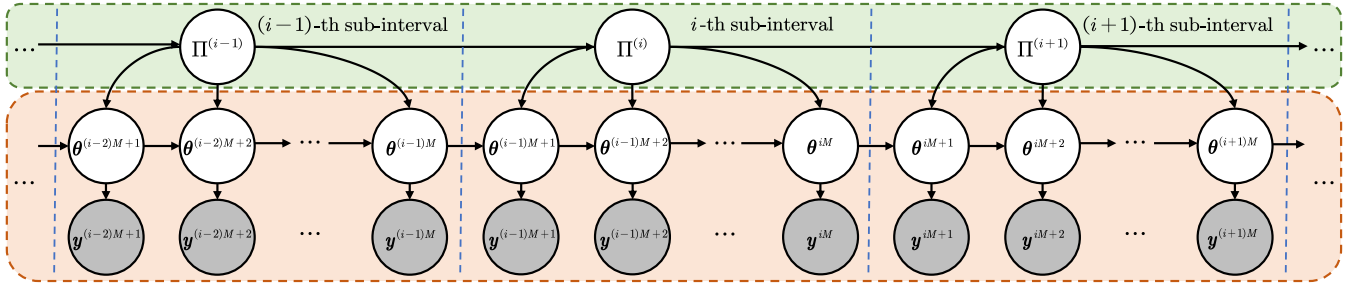


Figure 2: Graphical representation of the NS-PGDS. The time interval is divided into equally-spaced sub-intervals. Each sub-interval contains M time steps. The transition dynamics is stationary within a sub-interval. In particular, the transition matrices evolve over sub-intervals via Dirichlet Markov processes while latent factors evolve over time steps via Eq.(1).

proposed model allows the latent factors to evolve over time steps while the transition matrices change over sub-intervals but assumed to be stationary within each sub-interval, as shown in Figure 2. In particular, we let each sub-interval contains M time steps, and the i -th interval contains time steps $\{t \mid t = (i-1)M + 1, \dots, iM\}$. We define $i(t)$ as the function that maps time step t to its corresponding sub-interval.

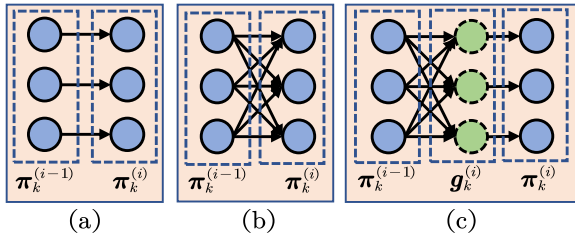


Figure 3: Diagrams of the proposed Dirichlet Markov constructions. (a) is the Dir-Dir construction. (b) is the Dir-Gam-Dir construction which takes mutation into account. (c) illustrates the PR-Gam-Dir construction which adopts Poisson randomized gamma distribution and can be equivalently represented as Eq.(6a) and Eq.(6b).

Dirichlet-Dirichlet Markov processes. To capture how the underlying transition kernel smoothly evolves over sub-intervals, we first propose the Dirichlet-Dirichlet (Dir-Dir) Markov chain structure as

$$\pi_k^{(i)} \mid \pi_k^{(i-1)} \sim \text{Dir} \left(\eta K \pi_{1k}^{(i-1)}, \dots, \eta K \pi_{Kk}^{(i-1)} \right), \quad (2)$$

where $\pi_k^{(i)}$ represents the k -th column of $\Pi^{(i)}$, and the prior of the scaling parameter η is given by $\eta \sim \text{Gam}(e_0, f_0)$.

The initial states are defined as $\theta_k^{(1)} \sim \text{Gam}(\tau_0 \nu_k, \tau_0)$. The prior for the transition kernel of the first sub-interval is given by $\pi_k^{(1)} \sim \text{Dir}(\nu_1 \nu_k, \dots, \xi \nu_k, \dots, \nu_K \nu_k)$, where $\nu_k \sim \text{Gam}(\frac{\gamma_0}{K}, \beta)$ and $\xi, \beta \sim \text{Gam}(\epsilon_0, \epsilon_0)$. Note that the expectation and variance of the transition kernel at i -th sub-interval can be calculated as

$$\begin{aligned} \mathbb{E} \left[\pi_k^{(i)} \mid \pi_k^{(i-1)} \right] &= \pi_k^{(i-1)}, \\ \text{Var} \left[\pi_{k_1 k}^{(i)} \mid \pi_k^{(i-1)} \right] &= \frac{\pi_{k_1 k}^{(i-1)} \left(1 - \pi_{k_1 k}^{(i-1)} \right)}{\eta K + 1}, \end{aligned}$$

respectively. The transition dynamics of i -th sub-interval inherits the information of the previous sub-interval, and also adapts to the data observed in the current sub-interval. The

scaling parameter η controls the variance of the transition matrices.

The prior specification defined in Eq.(2) by rescaling the transition matrix at the previous sub-interval allows the transition dynamics to change smoothly, and thus might be insufficient to capture the rapid changes observed in complicated dynamics. To further improve the flexibility of the transition structure, two modified Dirichlet Markov chains are studied to capture the correlation structure between the dimensions of the transition matrices over time.

Dirichlet-Gamma-Dirichlet Markov processes. We first introduce the Dirichlet-Gamma-Dirichlet (Dir-Gam-Dir) Markov chain to model the evolving transition matrices as

$$\begin{aligned} \pi_k^{(i)} &\sim \text{Dir} \left(\alpha_{1k}^{(i)}, \dots, \alpha_{Kk}^{(i)} \right), \\ \alpha_{k_1 k}^{(i)} &\sim \text{Gam} \left(\gamma_k^{(i-1)} \sum_{k_2=1}^K \psi_{kk_1 k_2}^{(i-1)} \pi_{k_2 k}^{(i-1)}, c_k^{(i)} \right), \end{aligned} \quad (3)$$

where we use $\psi_{kk_1 k_2}^{(i-1)}$ to capture the mutation between two consecutive sub-intervals, and its prior is given by

$$\begin{aligned} \left(\psi_{k_1 k_2}^{(i-1)}, \dots, \psi_{kK k_2}^{(i-1)} \right) &\sim \text{Dir}(\epsilon_0, \dots, \epsilon_0), \\ \gamma_k^{(i)}, c_k^{(i)} &\sim \text{Gam}(\epsilon_0, \epsilon_0). \end{aligned}$$

Compared with the construction defined by Eq.(2), the expectation of Dirichlet-Gamma-Dirichlet Markov chain is

$$\mathbb{E} \left[\pi_k^{(i)} \mid \pi_k^{(i-1)} \right] = \Psi_k^{(i-1)} \pi_k^{(i-1)}.$$

This construction takes interactions among components of columns into account. Hence it will dramatically improve the flexibility of our model and better fit more complicated dynamics, compared with Dir-Dir Markov chains that only yield smoothing transition dynamics.

Poisson-randomized-gamma-Dirichlet Markov processes. To further improve the expressiveness of the time-varying transition kernel, and to induce sparse patterns, we further define the Poisson-randomized-gamma-Dirichlet (PR-Gam-Dir) Markov chain as

$$\begin{aligned} \pi_k^{(i)} &\sim \text{Dir} \left(\alpha_{1k}^{(i)}, \dots, \alpha_{Kk}^{(i)} \right), \\ \alpha_{k_1 k}^{(i)} &\sim \text{RG1} \left(\epsilon^\alpha, \gamma_k^{(i-1)} \sum_{k_2=1}^K \psi_{kk_1 k_2}^{(i-1)} \pi_{k_2 k}^{(i-1)}, c_k^{(i)} \right), \end{aligned} \quad (4)$$

where $\text{RG1}(\cdot)$ denotes the randomized gamma distribution of the first type [Yuan and Kalbfleisch, 2000]. Similarly, for

$\psi_{kk_1k_2}^{(i-1)}$, $\gamma_k^{(i)}$, and $c_k^{(i)}$, the priors are given by

$$\begin{aligned} (\psi_{kk_1k_2}^{(i-1)}, \dots, \psi_{kKk_2}^{(i-1)}) &\sim \text{Dir}(\epsilon_0, \dots, \epsilon_0), \\ \gamma_k^{(i)}, c_k^{(i)} &\sim \text{Gam}(\epsilon_0, \epsilon_0), \text{ respectively.} \end{aligned}$$

The diagrams of three Dirichlet Markov constructions are shown in Figure 3.

4 Markov Chain Monte Carlo Inference

In this section, we present a fully-conjugate and efficient Gibbs sampler for the proposed NS-PGDS. The sampling algorithm depends on two data augmentation techniques, which we will repeatedly exploit, thus we list them below. Here we only illustrate the key points of the derivation and the details can be found in the supplementary material.

Lemma 1. *If $y \sim \text{NB}(a, g(\zeta))$ and $l \sim \text{CRT}(y, a)$, where $\text{NB}(\cdot)$ refers to negative binomial distribution, $\text{CRT}(\cdot)$ represents Chinese restaurant table distribution [Teh et al., 2006], and $g(z) = 1 - \exp(-z)$. Then the joint distribution of y and l can be equivalently distributed as $y \sim \text{SumLog}(l, g(\zeta))$ and $l \sim \text{Pois}(a\zeta)$ [Zhou and Carin, 2015], i.e.*

$$\begin{aligned} &\text{NB}(y; a, g(\zeta)) \text{CRT}(l; y, a) \\ &= \text{SumLog}(y; l, g(\zeta)) \text{Pois}(l; a\zeta), \end{aligned}$$

where $\text{SumLog}(l, g(\zeta)) = \sum_{i=1}^l x_i$ and $x_i \sim \text{Log}(g(\zeta))$ are independently and identically logarithmic distributed random variables [Johnson et al., 2005].

Lemma 2. *Suppose $\mathbf{n} = (n_1, \dots, n_K)$ and*

$$\mathbf{n} | n \sim \text{DirMult}(n, r_1, \dots, r_K),$$

where $\text{DirMult}(\cdot)$ refers to Dirichlet-multinomial distribution. We sample augmented variable $q | n \sim \text{Beta}(n, r)$, where $r = \sum_{k=1}^K r_k$. According to [Zhou, 2018], conditioning on q , we have $n_k \sim \text{NB}(r_k, q)$.

Sampling $y_{vk}^{(t)}$: Use the relationship between Poisson and multinomial distributions, we sample

$$\left((y_{vk}^{(t)})_{k=1}^K | - \right) \sim \text{Mult} \left(y_v^{(t)}, \left(\frac{\phi_{vk} \theta_k^{(t)}}{\sum_{k=1}^K \phi_{vk} \theta_k^{(t)}} \right)_{k=1}^K \right).$$

Sampling ϕ_k : Via Dirichlet-multinomial conjugacy, the posterior of ϕ_k is

$$(\phi_k | -) \sim \text{Dir} \left(\epsilon_0 + \sum_{t=1}^T y_{1k}^{(t)}, \dots, \epsilon_0 + \sum_{t=1}^T y_{V_k}^{(t)} \right).$$

Sampling $\theta_k^{(t)}$: To sample from the posterior of $\theta_k^{(t)}$, we first sample the auxiliary variables. Set $l_{\cdot k}^{(T+1)} = 0$ and $\zeta^{(T+1)} = 0$, sampling backwards from $t = T, \dots, 2$,

$$\begin{aligned} (l_{\cdot k}^{(t)} | -) &\sim \text{CRT} \left(y_{\cdot k}^{(t)} + l_{\cdot k}^{(t+1)}, \tau_0 \sum_{k_2=1}^K \pi_{kk_2}^{i(t-1)} \theta_{k_2}^{(t-1)} \right), \\ (l_{k_1}^{(t)}, \dots, l_{k_K}^{(t)} | -) &\sim \\ &\text{Mult} \left(l_{\cdot k}^{(t)}, \left(\frac{\pi_{k_1}^{i(t-1)} \theta_{k_1}^{(t-1)}}{\sum_{k_2=1}^K \pi_{kk_2}^{i(t-1)} \theta_{k_2}^{(t-1)}}, \dots, \frac{\pi_{k_K}^{i(t-1)} \theta_{k_K}^{(t-1)}}{\sum_{k_2=1}^K \pi_{kk_2}^{i(t-1)} \theta_{k_2}^{(t-1)}} \right) \right). \end{aligned}$$

Let us define

$$l_{\cdot k}^{(t)} = \sum_{k_1=1}^K l_{k_1 k}^{(t)} \text{ and } \zeta^{(t)} = \ln \left(1 + \frac{\delta^{(t)}}{\tau_0} + \zeta^{(t+1)} \right).$$

After sampling the auxiliary variables, then for $t = 1, \dots, T$, by Poisson-gamma conjugacy, we obtain

$$\begin{aligned} (\theta_k^{(1)} | -) &\sim \text{Gam} \left(y_{\cdot k}^{(1)} + l_{\cdot k}^{(2)} + \tau_0 \nu_k, \tau_0 + \delta^{(1)} + \zeta^{(2)} \tau_0 \right), \\ (\theta_k^{(t)} | -) &\sim \\ &\text{Gam} \left(y_{\cdot k}^{(t)} + l_{\cdot k}^{(t+1)} + \tau_0 \sum_{k_2=1}^K \pi_{kk_2}^{i(t-1)} \theta_{k_2}^{(t-1)}, \tau_0 + \delta^{(t)} + \zeta^{(t+1)} \tau_0 \right). \end{aligned}$$

Sampling $\Pi^{(i)}$: Here we only illustrate Gibbs sampling algorithm for PR-Gam-Dir construction, sampling algorithms for other constructions can be found in the supplementary material. We define M as the length of each interval, and I as the number of intervals. For $i = I, \dots, 2$, because $(l_{1k}^{(i)}, \dots, l_{Kk}^{(i)})$ and $(g_{\cdot 1k}^{(i+1)}, \dots, g_{\cdot Kk}^{(i+1)})$ are multinomial distributed, where $l_{k_1 k}^{(i)} = \sum_{(i-1)M+1}^{iM} l_{k_1 k}^{(t)}$ refers to the summation of $l_{k_1 k}^{(t)}$ over i -th interval. By the definition of Dirichlet-multinomial distribution and via Lemma 2, defining $g_{k_1 k}^{(I+1)} = 0$, we sample the auxiliary variables as $(q_k^{(i)} | -) \sim \text{Beta}(l_{\cdot k}^{(i)} + g_{\cdot k}^{(i+1)}, \alpha_{\cdot k}^{(i)})$. Via Lemma 2, we have $(l_{k_1 k}^{(i)} + g_{\cdot k_1 k}^{(i+1)}) \sim \text{NB}(\alpha_{k_1 k}^{(i)}, q_k^{(i)})$. Then we further sample $(h_{k_1 k}^{(i)} | -) \sim \text{CRT}(l_{k_1 k}^{(i)} + g_{\cdot k_1 k}^{(i+1)}, \alpha_{k_1 k}^{(i)})$. Via Lemma 1, we obtain

$$h_{k_1 k}^{(i)} \sim \text{Pois} \left(-\alpha_{k_1 k}^{(i)} \ln(1 - q_k^{(i)}) \right). \quad (5)$$

For Dirichlet-Randomized-Gamma-Dirichlet Markov construction defined by Eq.(4), we can equivalently represent it as

$$\alpha_{k_1 k}^{(i)} \sim \text{Gam} \left(g_{k_1 k}^{(i)} + \epsilon^\alpha, c_k^{(i)} \right), \quad (6a)$$

$$g_{k_1 k}^{(i)} = \text{Pois} \left(\gamma^{(i-1)} \sum_{k_2=1}^K \psi_{kk_1k_2}^{(i-1)} \pi_{k_2 k}^{(i-1)} \right). \quad (6b)$$

We define $\lambda_{k_1 k}^{(i-1)} \triangleq \gamma_k^{(i-1)} \sum_{k_2=1}^K \psi_{kk_1k_2}^{(i-1)} \pi_{k_2 k}^{(i-1)}$ for notation conciseness. By Poisson-gamma conjugacy and Eq.(5), we have

$$(\alpha_{k_1 k}^{(i)} | -) \sim \text{Gam} \left(g_{k_1 k}^{(i)} + \epsilon^\alpha + h_{k_1 k}^{(i)}, c_k^{(i)} - \ln(1 - q_k^{(i)}) \right).$$

If $\epsilon^\alpha > 0$, we can sample the posterior of $g_{k_1 k}^{(i)}$ via

$$(g_{k_1 k}^{(i)} | -) \sim \text{Bessel} \left(\epsilon^\alpha - 1, 2\sqrt{\alpha_{k_1 k}^{(i)} c_k^{(i)} \lambda_{k_1 k}^{(i-1)}} \right),$$

where $\text{Bessel}(\cdot)$ denotes Bessel distribution. If $\epsilon^\alpha = 0$, we sample $g_{k_1 k}^{(i)}$ via

$$(g_{k_1 k}^{(i)} | -) \sim \begin{cases} \text{Pois} \left(\frac{c_k^{(i)} \lambda_{k_1 k}^{(i-1)}}{c_k^{(i)} - \ln(1 - q_k^{(i)})} \right) & \text{if } h_{k_1 k}^{(i)} = 0 \\ \text{SCH} \left(h_{k_1 k}^{(i)}, \frac{c_k^{(i)} \lambda_{k_1 k}^{(i-1)}}{c_k^{(i)} - \ln(1 - q_k^{(i)})} \right) & \text{otherwise,} \end{cases}$$

where $\text{SCH}(\cdot)$ denotes the shifted confluent hypergeometric distribution [Schein *et al.*, 2019].

Defining $g_{k_1 k}^{(i)} = g_{k_1 \cdot k}^{(i)} = \sum_{k_2=1}^K g_{k_1 k_2 k}^{(i)}$, we first augment

$$\left(g_{k_1 1 k}^{(i)}, \dots, g_{k_1 K k}^{(i)} \right) \sim \text{Mult} \left(g_{k_1 k}^{(i)}, \left(\psi_{k k_1 k_2}^{(i-1)} \pi_{k_2 k}^{(i-1)} \right)_{k_2=1}^K \right).$$

Then we obtain $g_{k_1 k_2 k}^{(i)} \sim \text{Pois} \left(\gamma^{(i-1)} \psi_{k k_1 k_2}^{(i-1)} \pi_{k_2 k}^{(i-1)} \right)$. By Dirichlet-multinomial conjugacy, we have

$$\begin{aligned} \left(\left(\psi_{k k_1 k_2}^{(i-1)}, \dots, \psi_{k K k_2}^{(i-1)} \right) \mid - \right) &\sim \text{Dir} \left(\epsilon_0 + g_{1 k_2 k}^{(i)}, \dots, \epsilon_0 + g_{K k_2 k}^{(i)} \right), \\ \left(\pi_k^{(i-1)} \mid - \right) &\sim \\ \text{Dir} \left(\alpha_{1k}^{(i-1)} + l_{1k}^{(i-1)} + g_{\cdot 1 k}^{(i)}, \dots, \alpha_{Kk}^{(i-1)} + l_{Kk}^{(i-1)} + g_{\cdot K k}^{(i)} \right). \end{aligned}$$

Specifically, we have $\alpha_{k_1 k}^{(1)} = \nu_{k_1} \nu_k$, if $k_1 \neq k$, and $\alpha_{k_1 k}^{(1)} = \xi \nu_k$, if $k_1 = k$. Via Poisson-gamma conjugacy, we obtain

$$\left(\gamma_k^{(i-1)} \mid - \right) \sim \text{Gam} \left(\epsilon_0 + g_{\cdot k}^{(i)}, \epsilon_0 + 1 \right).$$

By gamma-gamma conjugacy, we have

$$\left(c_k^{(i)} \mid - \right) \sim \text{Gam} \left(\epsilon_0 + \gamma_k^{(i-1)}, \epsilon_0 + \sum_{k_1=1}^K \alpha_{k_1 k}^{(i)} \right).$$

5 Related Work

Modeling count time sequences has been receiving increasing attentions in statistical and machine learning communities. Han *et al.* [2014] adopted linear dynamical systems to capture the underlying dynamics of the data and leveraged Extended Rank likelihood function to model count observations. Some Poisson-gamma models assume that the count vector at each time step is modeled by Poisson factor analysis (PFA) [Zhou and Carin, 2015] and leverage special stochastic processes to model the temporal dependencies of latent factors. For example, gamma process dynamic Poisson factor analysis (GP-DPFA) [Acharya *et al.*, 2015] adopts gamma Markov chains which assumes the latent factor of the next time step is drawn from a gamma distribution with the shape parameter be the latent factor of the current time step. Schein *et al.* [2016b] proposed Poisson-gamma dynamical systems (PGDSs), which take the interactions among latent dimensions into account and use a transition matrix to capture the interactions. Deep dynamic Poisson factor analysis (DDPFA) [Gong and Huang, 2017] adopts recurrent neural networks (RNNs) to capture the complex long-term dependencies of latent factors. Yang and Koepl [2018a] applied Poisson-gamma count model to analyze relational data arising from longitudinal networks, which can capture the evolution of individual node-group memberships over time. Many modifications of PGDS have been proposed in recent years. Guo *et al.* [2018] proposed deep Poisson-gamma dynamical systems which aim to capture the long-range temporal dependencies. Schein *et al.* [2019] employed Poisson-randomized gamma distribution to build a new transition process of latent factors. Chen *et al.* [2021] proposed Switching Poisson-gamma dynamical systems (SPGDS), allowing PGDS to select from several transition matrices, and thus can better adapt to nonlinear dynamics. In contrast to SPGDS, the number of

transition matrices of the proposed NS-PGDS is not limited and thus can be adopted to analyze various complicated non-stationary count sequences. Filstroff *et al.* [2021] extensively analyzed many gamma Markov chains for non-negative matrix factorization and introduced new gamma Markov chains with well-defined stationary distribution (BGAR).

6 Experiments

We conducted experiments for both predictive and exploratory analysis to demonstrate the ability of the proposed model in capturing non-stationary count time sequences. The baseline models included in the experiments are: 1) Gamma process dynamic Poisson factor analysis (GP-DPFA) [Acharya *et al.*, 2015]. GP-DPFA models the evolution of latent components as $\theta_k^{(t)} \sim \text{Gam} \left(\theta_k^{(t-1)}, c_t \right)$, in which each component evolves independently of the other components. 2) Gamma Markov chains on the rate parameter of gamma distribution (GMC-RATE) [Filstroff *et al.*, 2021]. GMC-RATE adopts gamma Markov chains defined via the rate parameter of the gamma distribution to model the evolution of $\theta_k^{(t)}$ as $\theta_k^{(t)} \sim \text{Gam} \left(\alpha, \beta / \theta_k^{(t-1)} \right)$. 3) Gamma Markov chains on the rate parameter with hierarchical auxiliary variable (GMC-HIER) [Filstroff *et al.*, 2021]. GMC-HIER models the evolution of latent components with an auxiliary variable as $z_k^{(t)} \sim \text{Gam} \left(\alpha_z, \beta_z \theta_k^{(t-1)} \right)$ and $\theta_k^{(t)} \sim \text{Gam} \left(a_\theta, \beta_\theta z_k^{(t)} \right)$. 4) Autogressive beta-gamma processes (BGAR) [Lewis *et al.*, 1989; Filstroff *et al.*, 2021]. BGAR is also a gamma Markov model. In contrast to the above models, there is a well-defined stationary distribution for BGAR. 5) Poisson-gamma dynamical system (PGDS) [Schein *et al.*, 2016b] takes interactions among latent dimensions into account, and models the evolution of $\theta_k^{(t)}$ as $\theta_k^{(t)} \sim \text{Gam} \left(\tau_0 \sum_{k_2=1}^K \pi_{k k_2} \theta_{k_2}^{(t-1)}, \tau_0 \right)$.

The real-world datasets used in the experiments are: 1) **Integrated Crisis Early Warning System (ICEWS)**: ICEWS is an international relations event dataset, comprising interaction events between countries extracted from news corpora. For ICEWS dataset, we have $T = 365$ time steps and $V = 6197$ dimensions, and we set $M = 30$. 2) **NIPS**: NIPS dataset contains the papers published in the NeurIPS conference from 1987 to 2015. We have $T = 28$ time steps and $V = 2000$ dimensions for NIPS dataset and we set $M = 5$. 3) **U.S. Earthquake Intensity (USEI)**: USEI dataset contains a collection of damage and felt reports for U.S. (and a few other countries) earthquakes. We use the monthly reports from 1957-1986 and have $T = 348$, $V = 64$ and set $M = 34$. 4) **COVID-19**: COVID-19 dataset contains daily death cases data for states in the United States, spanning from March 2020 to June 2020. For this dataset, we have $V = 51$ dimensions and $T = 90$ time steps and set $M = 20$.

6.1 Predictive Analysis

To compare the predictive performance of the proposed model with the baselines, we considered two standard tasks: data smoothing and forecasting. For data smoothing task, our

			GP-DPFA	GMC-RATE	GMC-HIER	BGAR	PGDS	NS-PGDS (Dir-Dir)	NS-PGDS (Dir-Gam-Dir)	NS-PGDS (PR-Gam-Dir)
ICEWS	MAE	S	0.259 ±0.005	0.258 ±0.005	0.256 ±0.006	0.264 ±0.006	0.215 ±0.007	0.215 ±0.008	0.214 ±0.008	0.215 ±0.008
		F	0.176 ±0.005	0.187 ±0.003	0.185 ±0.016	0.222 ±0.043	0.185 ±0.003	0.167 ±0.009	0.169 ±0.006	0.169 ±0.009
	MRE	S	0.125 ±0.003	0.124 ±0.002	0.122 ±0.003	0.130 ±0.004	0.102 ±0.005	0.101 ±0.005	0.101 ±0.005	0.102 ±0.005
		F	0.099 ±0.006	0.114 ±0.003	0.111 ±0.018	0.142 ±0.036	0.108 ±0.001	0.094 ±0.005	0.097 ±0.004	0.097 ±0.008
NIPS	MAE	S	18.299 ±6.545	17.105 ±6.449	17.098 ±6.441	17.935 ±6.450	14.706 ±4.414	14.032 ±4.401	14.026 ±4.405	14.014 ±4.387
		F	48.355 ±1.461	46.234 ±1.629	102.506 ±39.932	62.449 ±14.463	51.562 ±0.679	45.979 ±1.342	46.710 ±1.152	46.582 ±1.196
	MRE	S	0.729 ±0.412	0.684 ±0.316	0.664 ±0.315	0.769 ±0.366	0.590 ±0.097	0.581 ±0.090	0.581 ±0.090	0.580 ±0.090
		F	0.415 ±0.016	0.387 ±0.023	0.580 ±0.148	0.465 ±0.049	0.459 ±0.006	0.399 ±0.003	0.395 ±0.006	0.397 ±0.003
USEI	MAE	S	4.681 ±0.564	4.931 ±0.872	4.748 ±0.829	5.244 ±0.939	4.703 ±0.538	4.600 ±0.542	4.608 ±0.541	4.596 ±0.562
		F	11.665 ±0.367	9.454 ±0.809	12.423 ±1.060	21.948 ±0.133	11.118 ±0.220	7.973 ±1.222	7.168 ±1.221	7.296 ±1.127
	MRE	S	1.458 ±0.177	1.128 ±0.189	1.088 ±0.162	1.941 ±0.209	1.279 ±0.257	1.309 ±0.220	1.298 ±0.236	1.301 ±0.229
		F	7.473 ±0.623	6.508 ±0.571	8.929 ±2.514	13.706 ±1.268	4.238 ±0.325	2.602 ±0.455	2.577 ±0.331	2.685 ±0.366
COVID-19	MAE	S	7.935 ±0.751	7.144 ±1.159	7.240 ±0.848	7.819 ±1.348	7.566 ±1.095	6.969 ±1.107	6.988 ±1.056	6.981 ±1.022
		F	9.137 ±1.102	9.600 ±1.257	10.409 ±1.910	12.550 ±2.156	9.314 ±0.236	8.799 ±0.706	8.770 ±0.438	9.033 ±0.477
	MRE	S	0.564 ±0.126	0.493 ±0.136	0.504 ±0.109	0.769 ±0.169	0.558 ±0.130	0.523 ±0.125	0.525 ±0.124	0.526 ±0.123
		F	0.627 ±0.106	0.556 ±0.052	0.585 ±0.067	0.759 ±0.150	0.585 ±0.007	0.523 ±0.028	0.519 ±0.017	0.513 ±0.014

Table 1: Results of predictive analysis. "S" means data smoothing and "F" means data forecasting.

objective is to predict $\mathbf{y}^{(t)}$ given the remaining data observation $\mathbf{Y} \setminus \mathbf{y}^{(t)}$. To this end, we randomly masked 10 percents of the observed data over non-adjacent time steps, and predicted the masked values. For forecasting task, we held out data of the last S time steps, and predicted $\mathbf{y}^{(T+1)}, \dots, \mathbf{y}^{(T+S)}$ given $\mathbf{y}^{(1)}, \dots, \mathbf{y}^{(T)}$. In this experiment we set $S = 2$. We ran the baseline models including GP-DPFA, PGDS, GMC-RATE, GMC-HIER, BGAR, using their default settings as provided in [Acharya *et al.*, 2015; Schein *et al.*, 2016b; Filstroff *et al.*, 2021]. For NS-PGDS, we set $K = 100$ for ICEWS, $K = 10$ for other datasets, and set $\tau_0 = 1, \gamma_0 = 50, \epsilon_0 = 0.1$. We performed 4000 Gibbs sampling iterations. In the experiments, we found that the Gibbs sampler started to converge after 1000 iterations, and thus we set the burn-in time be 2000 iterations. We retained every hundredth sample, and averaged the predictions over the samples. Mean relative error (MRE) and mean absolute error (MAE) are adopted to evaluate the model’s predictive capability, which are defined as $\text{MRE} = \frac{1}{TV} \sum_t \sum_v \frac{|y_v^{(t)} - \hat{y}_v^{(t)}|}{1 + y_v^{(t)}}$ and $\text{MAE} = \frac{1}{TV} \sum_t \sum_v |y_v^{(t)} - \hat{y}_v^{(t)}|$ respectively, where $y_v^{(t)}$ indicates the true count and $\hat{y}_v^{(t)}$ is the prediction.

As the experiment results shown in Table 1, NS-PGDS exhibits improved performance in both data smoothing and forecasting tasks. We attribute this enhanced capability to the time-varying transition kernels, which effectively adapt to the non-stationary environment, and thus achieve improved predictive performance.

6.2 Exploratory Analysis

We used ICEWS and NIPS datasets for exploratory analysis, and chose NS-PGDS with Dirichlet-Dirichlet Markov chains for illustration. Figure 4(a) and Figure 4(b) demonstrate the top 2 latent factors inferred by NS-PGDS from ICEWS dataset. From Figure 4(a) we can see that the main labels are "Iraq (IRQ)–United States (USA)", "Iraq (IRQ)–United Kingdom (UK)", "Russia (RUS)–United States (USA)", and so on. This latent factor probably corresponds to the topic about Iraq war. Besides, in Figure 4(a), there is a peak around

March, 2003, and we know that the Iraq war broke out exactly on 20 March, 2003. In addition, the most dominant labels shown in Figure 4(b) are "Japan (JPN)–United States (USA)", "China (CHN)–United States (USA)", "North Korea (PRK)–United States (USA)", "South Korea (KOR)–United States (USA)", and so on. We can infer that this latent factor corresponds to "Six-Party Talks" and other accidents about it.

Figure 4(c) demonstrates the evolving trends of the top 5 latent factors inferred by NS-PGDS from NIPS dataset, and the legend indicates the representative words of the corresponding latent factors. Clearly, the green and blue lines correspond to the latent factors of neural network research which started to decline from the 1990s. From the 1990s we see that the latent factors about statistical and probabilistic methods began to dominate the NeurIPS conference. In addition, NS-PGDS also captured the revival of neural networks (blue line) from the 2010s. The above observations from the latent structure inferred by NS-PGDS match our prior knowledge.

Next, we explored the time-varying transition matrices inferred by NS-PGDS. We chose NIPS dataset for illustration, and set $K = 10$ and the interval length M to be 5. The time-varying transition matrices are shown from Figure 5(b) to Figure 5(f). At the beginning, matrices shown in Figure 5(b) and Figure 5(c) are close to identity matrices. Then the transition matrices tend to become block diagonal matrices with 2 blocks, as shown in Figure 5(d)–5(f). The representative words for latent factors in the first block are "state-linear-classification", "network-neural-networks", "kernel-image-space", "network-neural-networks", "neural-networks-state". The representative words for latent factors in the second block are "image-sparse-matrix", "kernel-supervised-random", "matrix-sample-random", "inference-prior-latent", "state-policy-gamma". The first block primarily captured the correlations among the research topics about neural networks. The second block reflects that, from the 1990s, statistical learning and Bayesian methods began to dominate, and these topics are highly correlated. Figure 5(a) illustrates the transition matrix inferred by the PGDS, which is averaged over all time steps. Compared with the

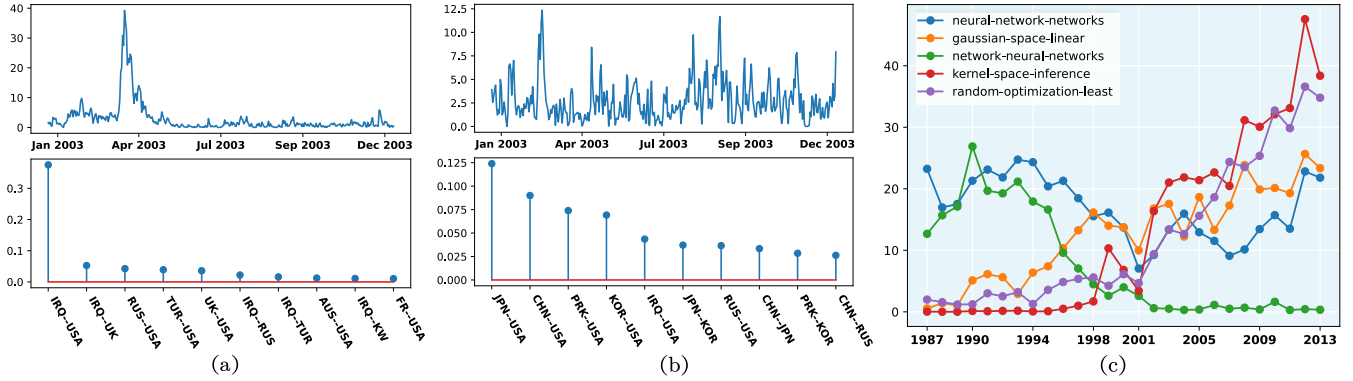


Figure 4: Latent factors inferred by NS-PGDS. (a) and (b) illustrate the top 2 latent factors inferred from ICEWS dataset, (a) corresponds to Iraq war and (b) corresponds to the Six-Party Talks. (c) illustrates the evolving trends of the top 5 latent factors inferred from NIPS dataset.

NS-PGDS, the PGDS can not capture the informative time-varying transition dynamics.

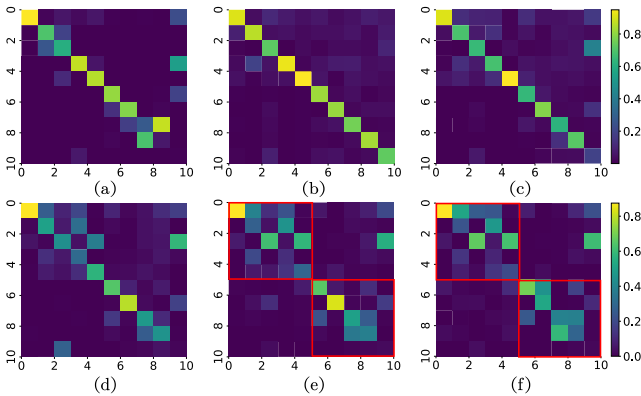


Figure 5: Transition matrices inferred from NIPS dataset. (a) illustrates the transition matrix inferred by the PGDS. (b)-(f) illustrate the time-varying transition matrices inferred by the NS-PGDS.

We also analyzed the features of the proposed Dirichlet Markov chains. The left column of Figure 6 demonstrates transition matrices of the first four sub-intervals of ICEWS dataset inferred by NS-PGDS (Dir-Dir). Because of the Dir-Dir construction, the consecutive transition matrices smoothly change over time and thus NS-PGDS may lack sufficient flexibility to capture rapid dynamics. The middle column of Figure 6 illustrates the transition matrices inferred by NS-PGDS (Dir-Gam-Dir), which takes mutations among latent components into account and captured more complicated patterns. Transition matrices inferred by PR-Gam-Dir construction are shown in the right column of Figure 6, these matrices not only exhibited sufficient flexibility but also captured sparser patterns compared with Dir-Gam-Dir construction.

7 Conclusion

The Poisson-gamma dynamical systems with time-varying transition matrices, have been proposed to capture complicated dynamics observed in *non-stationary* count sequences. In particular, Dirichlet Markov chains are constructed to allow the underlying transition matrices to evolve over time. Although the Dirichlet Markov processes lack conjugacy,

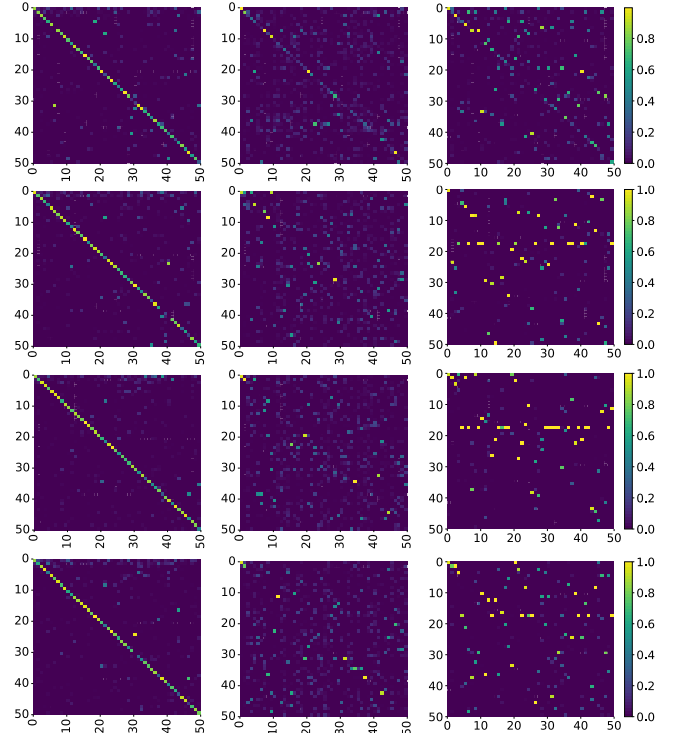


Figure 6: From top to bottom are the first four transition matrices inferred by different Dirichlet Markov chains from ICEWS dataset. Left column: Matrices inferred by Dir-Dir construction. Middle column: Matrices inferred by Dir-Gam-Dir construction. Right column: Matrices inferred by PR-Gam-Dir construction.

we have developed tractable-but-efficient Gibbs sampling algorithms to perform posterior simulation. The experiment results demonstrate the improved performance of the proposed NS-PGDS in data smoothing and forecasting tasks, compared with the PGDS with a stationary transition kernel. Moreover, the experimental results on several real-world data sets show the explainable structures inferred by the proposed NS-PGDS. In the future research, we consider to generalize Dirichlet belief networks by incorporating the proposed Dirichlet Markov chain constructions, which allow the hierarchical topics to mutate across layers, and thus can generate more richful text information. We also consider to capture

non-stationary interaction dynamics among individuals over online social networks [Yang and Koepl, 2018c; Yang and Koepl, 2018b; Yang and Koepl, 2020; Yang and Zha, 2023; Yang and Zha, 2024] in the future research.

References

- [Acharya *et al.*, 2015] Ayan Acharya, Joydeep Ghosh, and Mingyuan Zhou. Nonparametric bayesian factor analysis for dynamic count matrices. In *Artificial Intelligence and Statistics*, pages 1–9, 2015.
- [Blei and Lafferty, 2006] David M Blei and John D Lafferty. Dynamic topic models. In *Proceedings of the 23rd international conference on Machine learning*, pages 113–120, 2006.
- [Chang and Blei, 2009] Jonathan Chang and David Blei. Relational topic models for document networks. In *Proceedings of the Twelfth International Conference on Artificial Intelligence and Statistics*, pages 81–88, 2009.
- [Chen *et al.*, 2021] Wenchao Chen, Bo Chen, Yicheng Liu, Qianru Zhao, and Mingyuan Zhou. Switching poisson gamma dynamical systems. In *Proceedings of the Twenty-Ninth International Conference on International Joint Conferences on Artificial Intelligence*, pages 2029–2036, 2021.
- [Feng *et al.*, 2021] Luzhao Feng, Ting Zhang, Qing Wang, Yiran Xie, Zhibin Peng, Jiandong Zheng, Ying Qin, Muli Zhang, Shengjie Lai, Dayan Wang, et al. Impact of covid-19 outbreaks and interventions on influenza in china and the united states. *Nature communications*, 12(1):3249, 2021.
- [Filstroff *et al.*, 2021] Louis Filstroff, Olivier Gouvert, Cédric Févotte, and Olivier Cappé. A comparative study of gamma markov chains for temporal non-negative matrix factorization. *IEEE Transactions on Signal Processing*, 69:1614–1626, 2021.
- [Ghahramani and Roweis, 1998] Zoubin Ghahramani and Sam T Roweis. Learning nonlinear dynamical systems using an em algorithm. In *Proceedings of the 11th International Conference on Neural Information Processing Systems*, pages 431–437, 1998.
- [Gong and Huang, 2017] Chengyue Gong and Win-bin Huang. Deep dynamic poisson factorization model. In *Proceedings of the 31st International Conference on Neural Information Processing Systems*, pages 1665–1673, 2017.
- [Grossman *et al.*, 2020] Guy Grossman, Soojong Kim, Jonah M Rexer, and Harsha Thirumurthy. Political partisanship influences behavioral responses to governors’ recommendations for covid-19 prevention in the united states. *Proceedings of the National Academy of Sciences*, 117(39):24144–24153, 2020.
- [Guo *et al.*, 2018] Dandan Guo, Bo Chen, Hao Zhang, and Mingyuan Zhou. Deep poisson gamma dynamical systems. In *Proceedings of the 32nd International Conference on Neural Information Processing Systems*, pages 8451–8461, 2018.
- [Han *et al.*, 2014] Shaobo Han, Lin Du, Esther Salazar, and Lawrence Carin. Dynamic rank factor model for text streams. In *Proceedings of the 27th International Conference on Neural Information Processing Systems-Volume 2*, pages 2663–2671, 2014.
- [Jähnichen *et al.*, 2018] Patrick Jähnichen, Florian Wenzel, Marius Kloft, and Stephan Mandt. Scalable generalized dynamic topic models. In *International Conference on Artificial Intelligence and Statistics*, pages 1427–1435, 2018.
- [Johnson *et al.*, 2005] Norman L Johnson, Adrienne W Kemp, and Samuel Kotz. *Univariate discrete distributions*, volume 444. John Wiley & Sons, 2005.
- [Kalantari and Zhou, 2020] Rahi Kalantari and Mingyuan Zhou. Graph gamma process generalized linear dynamical systems. *arXiv preprint arXiv:2007.12852*, 2020.
- [Kalman, 1960] R. E. Kalman. A New Approach to Linear Filtering and Prediction Problems. *Journal of Basic Engineering*, 82(1):35–45, 1960.
- [Lewis *et al.*, 1989] Peter AW Lewis, Edward McKenzie, and David Kennedy Hugus. Gamma processes. *Stochastic Models*, 5(1):1–30, 1989.
- [Raymer *et al.*, 2013] James Raymer, Arkadiusz Wiśniowski, Jonathan J Forster, Peter WF Smith, and Jakub Bijak. Integrated modeling of european migration. *Journal of the American Statistical Association*, 108(503):801–819, 2013.
- [Schein *et al.*, 2015] Aaron Schein, John Paisley, David M Blei, and Hanna Wallach. Bayesian poisson tensor factorization for inferring multilateral relations from sparse dyadic event counts. In *Proceedings of the 21th ACM SIGKDD International conference on knowledge discovery and data mining*, pages 1045–1054, 2015.
- [Schein *et al.*, 2016a] Aaron Schein, Mingyuan Zhou, David Blei, and Hanna Wallach. Bayesian poisson tucker decomposition for learning the structure of international relations. In *International Conference on Machine Learning*, pages 2810–2819, 2016.
- [Schein *et al.*, 2016b] Aaron Schein, Mingyuan Zhou, and Hanna Wallach. Poisson-gamma dynamical systems. In *Proceedings of the 30th International Conference on Neural Information Processing Systems*, pages 5012–5020, 2016.
- [Schein *et al.*, 2019] Aaron Schein, Scott W Linderman, Mingyuan Zhou, David M Blei, and Hanna Wallach. Poisson-randomized gamma dynamical systems. In *Proceedings of the 33rd International Conference on Neural Information Processing Systems*, pages 782–793, 2019.
- [Sheldon and Dietterich, 2011] Daniel Sheldon and Thomas G Dietterich. Collective graphical models. In *Proceedings of the 24th International Conference on Neural Information Processing Systems*, pages 1161–1169, 2011.
- [Team, 2021] IHME COVID-19 Forecasting Team. Modeling covid-19 scenarios for the united states. *Nature medicine*, 27(1):94–105, 2021.

- [Teh *et al.*, 2006] Yee Whye Teh, Michael I Jordan, Matthew J Beal, and David M Blei. Hierarchical dirichlet processes. *Journal of the American Statistical Association*, 101(476):1566–1581, 2006.
- [Unwin *et al.*, 2020] H Juliette T Unwin, Swapnil Mishra, Valerie C Bradley, Axel Gandy, Thomas A Mellan, Helen Coupland, Jonathan Ish-Horowicz, Michaela AC Vollmer, Charles Whittaker, Sarah L Filippi, et al. State-level tracking of covid-19 in the united states. *Nature Communications*, 11(1):1–9, 2020.
- [Wang and McCallum, 2006] Xuerui Wang and Andrew McCallum. Topics over time: a non-markov continuous-time model of topical trends. In *Proceedings of the 12th ACM SIGKDD international conference on Knowledge discovery and data mining*, pages 424–433, 2006.
- [Wanner, 2021] Philippe Wanner. How well can we estimate immigration trends using google data? *Quality & Quantity*, 55(4):1181–1202, 2021.
- [Wilson, 2017] Tom Wilson. Methods for estimating sub-state international migration: The case of australia. *Spatial Demography*, 5(3):171–192, 2017.
- [Winkelmann, 2008] Rainer Winkelmann. *Econometric Analysis of Count Data*. Springer Publishing Company, Incorporated, 5th edition, 2008.
- [Yang and Koepl, 2018a] Sikun Yang and Heinz Koepl. Dependent relational gamma process models for longitudinal networks. In *International Conference on Machine Learning*, pages 5551–5560, 2018.
- [Yang and Koepl, 2018b] Sikun Yang and Heinz Koepl. Dependent relational gamma process models for longitudinal networks. In *Proceedings of the International Conference on Machine Learning (ICML)*, pages 5551–5560, 2018.
- [Yang and Koepl, 2018c] Sikun Yang and Heinz Koepl. A Poisson gamma probabilistic model for latent node-group memberships in dynamic networks. In *Proceedings of the AAAI Conference on Artificial Intelligence (AAAI)*, pages 4366–4373, 2018.
- [Yang and Koepl, 2020] Sikun Yang and Heinz Koepl. The Hawkes edge partition model for continuous-time event-based temporal networks. In *Proceedings of the 36th Conference on Uncertainty in Artificial Intelligence (UAI)*, pages 460–469, 2020.
- [Yang and Zha, 2023] Sikun Yang and Hongyuan Zha. Estimating latent population flows from aggregated data via inverting multi-marginal optimal transport. In *Proceedings of the 2023 SIAM International Conference on Data Mining (SDM)*, pages 181–189, 2023.
- [Yang and Zha, 2024] Sikun Yang and Hongyuan Zha. A variational autoencoder for neural temporal point processes with dynamic latent graphs. In *Proceedings of the AAAI Conference on Artificial Intelligence (AAAI)*, 2024.
- [Yuan and Kalbfleisch, 2000] Lin Yuan and John D Kalbfleisch. On the bessel distribution and related problems. *Annals of the Institute of Statistical Mathematics*, 52:438–447, 2000.
- [Zhou and Carin, 2012] M Zhou and L Carin. Augment-and-conquer negative binomial processes. *Advances in Neural Information Processing Systems*, 4:2546–2554, 2012.
- [Zhou and Carin, 2015] Mingyuan Zhou and Lawrence Carin. Negative binomial process count and mixture modeling. *IEEE Transactions on Pattern Analysis & Machine Intelligence*, 37(02):307–320, 2015.
- [Zhou, 2018] Mingyuan Zhou. Nonparametric bayesian negative binomial factor analysis. *Bayesian Analysis*, 13(4):1065–1093, 2018.